

An analysis of convective transport and parameter sensitivity in a single column version of the Goddard Earth Observation System, Version 5, General Circulation Model

L. E. Ott^a
J. Bacmeister^b
S. Pawson^c
K. Pickering^d
G. Stenchikov^e
M. Suarez^c
H. Huntrieser^f
M. Loewenstein^g
J. Lopez^h
I. Xueref-Remyⁱ

a. NASA Postdoctoral Program Fellow, Global Modeling and Assimilation Office, NASA GSFC, Greenbelt, Maryland

b. Goddard Earth Sciences and Technology Center, University of Maryland, Baltimore County, Baltimore, Maryland

c. Global Modeling and Assimilation Office, NASA GSFC, Greenbelt, Maryland

d. NASA GSFC, Greenbelt, Maryland

e. Department of Environmental Sciences, Rutgers University, New Brunswick, New Jersey

f. Institut für Physik der Atmosphäre, Deutsches Zentrum für Luft- und Raumfahrt, Oberpfaffenhofen, Germany

g. NASA ARC, Moffett Field, California

h. Bay Area Environmental Research Institute, Sonoma, California

i. Institut Pierre Simon Laplace, Laboratoire des Sciences du Climat et de l'Environnement, UMR CEA/CNRS 1572, Gif-sur-Yvette, Cedex, France

Abstract

Convection strongly influences the distribution of atmospheric trace gases. General circulation models (GCMs) use convective mass fluxes calculated by parameterizations to transport gases, but the results are difficult to compare with trace gas observations because of differences in scale. The high resolution of cloud-resolving models (CRMs) facilitates direct comparison with aircraft observations. Averaged over a sufficient area, CRM results yield a validated product directly comparable to output from a single global model grid column. This study presents comparisons of vertical profiles of convective mass flux and trace gas mixing ratios between CRM and single column model (SCM) simulations of storms observed during three field campaigns. In all three cases, SCM simulations underpredicted convective mass flux relative to CRM simulations. As a result, the SCM simulations produced lower trace gas mixing ratios in the upper troposphere in two of the three storms than did CRM simulations.

The impact of parameter sensitivity in the moist physics schemes employed in the SCM has also been examined. Statistical techniques identified the most significant parameters influencing convective transport. Results show that altered parameter settings can substantially improve the comparison between SCM and CRM convective mass flux. Upper tropospheric trace gas mixing ratios were also improved in two storms. In the remaining storm, the SCM representation of CO₂ was not improved because of differences in entrainment and detrainment levels in the CRM and SCM simulations. Trace gas observations provide an additional constraint which can be used to improve the representation of physical processes in GCMs.

1. Introduction

Convective transport profoundly affects both the vertical and horizontal distributions of trace gases in the atmosphere. Updrafts associated with convective clouds can rapidly transport species from the boundary layer to the middle and upper troposphere where atmospheric residence times are increased and horizontal winds are stronger. As a result, trace gases may be transported greater distances from source regions than if they remained in the boundary layer (e.g. Dickerson et al., 1987; Pickering et al., 1996; Bey et al., 2001). Stenchikov et al. [1996] showed that mixing across the tropopause resulting from strong convective events alters the composition of both the upper troposphere and lower stratosphere. In order for global models of the atmosphere to realistically simulate trace gas distributions, convective processes must be adequately represented. General circulation models (GCMs) and global chemistry-transport models (CTMs) use convective mass fluxes calculated by convective parameterizations to transport trace gases, but the results can be difficult to evaluate due to a lack of information about the chemical environment within clouds. Satellite observations are often limited by resolution as well as an inability to see through clouds. Aircraft observations obtained during field projects provide valuable information on the vertical distribution of trace gases in convective clouds but are difficult to relate to global models due to differences in scale.

Cloud-resolving models (CRMs) have the potential to bridge the gap between aircraft measurements, which are taken with a high temporal (~ 1 s) and spatial resolution (~ 100 m), and global model grid cells, which may be hundreds of kilometers wide. Interpreting aircraft observations taken in the vicinity of convective clouds requires an understanding of when and where in relation to the storm the observations were taken.

In- and out-of-cloud observations may represent significantly different chemical environments due to convective updrafts, wet scavenging, and cloud-enhanced photolysis rates (Madronich, 1987). Even at a constant altitude within a convective cloud, aircraft observations of trace gas mixing ratios may exhibit large variations depending on the region of the cloud sampled. Observations of gases emitted near the surface are typically greatest in the updraft core region where the least mixing with environmental air has occurred while observations taken in the storm anvil represent air parcels which have experienced a greater degree of dilution. This spatial distribution is evident in CRM studies of convective transport by Ott et al. [2007] and Barth et al. [2007a]. Transport calculated by CRMs can be validated by comparing in-cloud chemical measurements with model output sampled in regions of the domain which best represent the time and location of observation. For example, in a CRM intercomparison study by Barth et al. [2007b], two constant altitude anvil transects were used to compare observations with model results while DeCaria et al. [2005] sampled model output within a 160 km² region downwind of the storm core for comparison with data collected during a spiraling aircraft ascent through the anvil. In addition to providing detailed information about trace gas distributions in regions which were sampled, CRMs also provide information on regions which were not sampled or in which observations may be sparse. Unlike CRMs, a GCM employing a parameterized representation of convection is not capable of providing separate profiles of in- and out-of-cloud trace gas mixing ratios or information on subgrid scale variability which makes direct comparison with aircraft observations difficult.

Folkens et al. [2006] noted that the disparity in mass flux profiles produced by different parameterizations shows the need for additional observational constraints and used tropical climatologies of water vapor and trace gases compiled from satellite,

aircraft, and balloon-based observations to evaluate convective outflow characteristics produced by several parameterizations. The meteorological and thermodynamic properties of convection in GCMs have been studied by comparing CRM simulations with results from a single column model (SCM) version of a parent GCM (e.g. Bechtold et al., 2000; Ryan et al., 2000; Luo et al., 2006). This paper extends that technique to evaluate trace gas distributions simulated with an SCM against those simulated for three storms using a CRM. The high resolution of the CRM simulations allows the results to be compared with radar observations and in-cloud chemical measurements from aircraft to ensure that both the dynamic and chemical environment of the CRM simulated storms is reasonable (Ott et al., 2007). CRM output is averaged over an area comparable to a global model grid cell and compared with SCM results to evaluate the representation of convection in the SCM.

In addition to comparisons of trace gas distributions computed by CRMs and a SCM, the issue of parameter sensitivity in the SCM's moist physics is examined. The SCM evaluated here is from a version of the Goddard Earth Observing System, Version 5 (GEOS-5) GCM, which includes the relaxed Arakawa-Schubert (RAS) convection code (Moorthi and Suarez, 1992) with microphysics. Bacmeister et al. [2006] showed the importance of parameter settings in this module in determining precipitation patterns in a GCM. The impact on trace gas profiles has not previously been examined. The goal of these parameter sensitivity studies is to identify the most important parameters in controlling convective transport of trace gases. An ensemble of 3D simulations with perturbations to these parameters will be constructed in order to represent the uncertainty in trace gas distributions introduced by uncertainties in convective schemes.

Section 2 of this paper provides background on the models used in these studies.

In section 3, the CRM and SCM simulations of three thunderstorms observed during different field projects are described. Section 4 contains the method and results of a parameter sensitivity analysis and section 5 presents a summary and conclusions which may be drawn from this work.

2. Models

2.1. Cloud-resolving models

Two thunderstorms were simulated using the 3D Goddard Cumulus Ensemble Model (GCE) (Tao and Simpson, 1993; Tao et al., 2003a) and a third with the NASA Goddard version of the non-hydrostatic PSU/NCAR (MM5) mesoscale model (Tao et al., 2003b) run in cloud-resolving mode. All simulations were conducted employing a 2 km horizontal and a 0.5 km vertical resolution. Output from the GCE and MM5 were used to drive a 3-D Cloud-Scale Chemical Transport Model (CSCTM) developed at the University of Maryland and fully detailed in DeCaria [2000] and DeCaria et al. [2005]. Temperature, density, wind, hydrometeor (rain, snow, graupel, cloud water, and cloud ice), and diffusion coefficient fields from the cloud model simulation are read into the CSCTM every five or ten minutes in the simulation, and these fields are then interpolated to the model time step of 15 seconds. The transport of chemical tracers is calculated using a van Leer advection scheme.

2.2. GEOS-5 SCM

The GEOS-5 AGCM is a central component of the GEOS-5 atmospheric data assimilation system [Rienecker et al., 2007], where it is used for meteorological analysis and forecasting [Zhu and Gelaro, 2007]. It is also being adapted as a tool for studying composition and climate, for which an understanding of transport is required. The moist processes in GEOS-5 include a convective parameterization and prognostic cloud scheme

which are fully detailed in Bacmeister [2005]. Convection is parameterized using the relaxed Arakawa-Schubert (RAS) scheme of Moorthi and Suarez [1992], a modified version of the Arakawa-Schubert scheme [Arakawa and Schubert, 1974], in which the atmosphere is relaxed towards equilibrium. RAS represents convection as a sequence of linearly entraining plumes whose bases are defined as the lifting condensation level but which detrain at different levels. All levels between the cloud base and 100 hPa are tested for the possibility of convection. The cloud-base mass flux is calculated for each plume using a convective available potential energy based closure. On the basis of the cloud-base mass flux, the environmental temperature and moisture profiles are modified by each plume with the subsequent plumes receiving the modified sounding to represent the interaction between clouds of different heights which might coexist within the area covered by a typical GCM grid cell.

RAS calculates profiles of convective ice and liquid condensate within supersaturated plumes by reducing humidity by the amount necessary to achieve saturation. The prognostic cloud scheme contained in GEOS-5 calculates large-scale ice and liquid condensate by assuming a probability distribution function (pdf) of total water. Condensate is removed from the domain by evaporation, auto-conversion of liquid condensate, sedimentation of frozen condensate, and accretion of condensate by falling precipitation. The moist physics scheme recognizes three distinct types of precipitation or “showers” – that contained within convective updrafts, that originating from convective anvil clouds, and that originating from non-convective large-scale clouds. Due to the complicated subgrid geometry of convective clouds, the evolution of precipitation in these settings is difficult to parameterize in a GCM. In an effort to capture this complexity we have introduced several “tunable” parameters to the rain re-

evaporation scheme in the model. CNV_ENVF specifies a fraction of convective precipitation that is assumed to fall through the environment and may thus be exposed to re-evaporation in unsaturated environmental air. The area parameters CNV_BETA and ANV_BETA relate a diagnosed updraft or cloud areal fraction to an areal fraction of precipitation. This controls the diagnosed intensity of precipitation and, thereby, microphysical parameters derived from the Marshall-Palmer size distribution. Finally, an ad hoc, bulk scaling - BASE_REVAP_FAC - with a value from 0 to 1, is applied to the estimated re-evaporation.

The GEOS-5 SCM includes the same physical parameterizations and treatment of moist processes as the 3D AGCM. In these studies, the convective transport of tracer species was calculated online. Tracer profiles are successively modified by convective plumes within the RAS scheme in the same way as temperature and moisture. Turbulent mixing in the boundary layer is computed using the Lock et al. [2000] scheme in unstable conditions or when a cloud-topped boundary layer exists. In other conditions, the first-order scheme of Louis [1979] is applied.

SCM simulations of storms were initialized with profiles of temperature, wind, and moisture. To ensure consistency with the CRM simulated meteorology, these profiles were calculated by averaging CRM output over a 150 km by 150 km region of the domain in which convection occurred. Profiles of horizontal and vertical advective tendencies of temperature, moisture, and tracer mixing ratios were also computed from CRM output following the method of Waliser et al. [2002] and used to force the SCM. Vertical advective tendencies, which represent the impact of large-scale vertical motion on the SCM domain, were computed by subtracting a quantity representing the contribution of small scale vertical motions, such as those found in convective regions,

from an area-mean quantity (Waliser et al., 2002). The horizontal resolution of the SCM is dictated by the area over which initial and forcing conditions were computed which, in this study, is 150 km by 150 km. There are 40 vertical levels including 8 below 850 hPa. All storms were simulated with a time step of 30 minutes.

3. Case studies

3.1. The July 21 EULINOX storms

The EULINOX field campaign [Höller and Schumann, 2000; Huntrieser et al., 2002] was conducted in central Europe during June and July 1998 with the goal of better understanding convective transport of trace gases and lightning NO_x production. During the project, airborne measurements of chemical species and meteorological properties were collected by the Deutsches Zentrum für Luft- und Raumfahrt (DLR) Falcon and the Do228 research aircraft. The Do228 flew primarily in the boundary layer and lower troposphere below 4 km, while the Falcon investigated the upper troposphere and performed a number of anvil penetrations through monitored thunderstorms. Both radar and satellite observations were used to monitor the development of thunderstorms in the region. On the evening of July 21, 1998, the evolution of a severe thunderstorm west of Munich, Germany was observed as part of the EULINOX campaign and is documented in Höller et al. [2000]. The storm began as a single cell at approximately 1600 UTC and after an initial period of intensification, the storm split into two distinct cells observed on radar at 1652 UTC. The northernmost cell became multicellular in structure and was observed to decay soon after the cell-splitting event, while the southern cell intensified.

The GCE and CSCTM simulations of the July 21 EULINOX storm are fully described in Ott et al. [2007]. The 3-hour GCE simulation was successful in reproducing a number of observed storm features including the cell-splitting event. Simulated cloud

top heights were typically 14 km, which compared favorably with observations [Höller et al., 2000] and a MM5 simulation of the same storm presented by Fehr et al. [2004]. The GCE simulation was also able to reasonably reproduce vertical velocities calculated from an analysis of dual-Doppler radar observations of the southern storm. An initial condition profile of CO₂ was constructed using data from the Falcon ascent and a value of 355 ppbv above the tropopause from Strahan et al. [1998]. A comparison of simulated and observed in-cloud CO₂ and O₃ mixing ratios showed that the model was able to reasonably represent convective transport of tracer species.

Xu [1995] used the horizontal distributions of maximum cloud draft strength below the melting level and precipitation rate as criteria to partition a CRM domain into convective, stratiform, and cloud-free regions. Updraft convective mass flux was calculated by considering upward vertical motion in convective grid cells classified as saturated by the sum of cloud ice and water mixing ratios. The methods of Xu [1995] were used to define convective regions in the CRM domain and to calculate the updraft convective mass flux in all three CRM simulations. The SCM was run for three hours using initial condition and advective tendency profiles derived from the CRM output. Convective mass flux was averaged over 150 minutes of the SCM and CRM simulations, neglecting the first 30 minutes, which are considered to be spin-up. A comparison of the time averaged updraft convective mass fluxes (Fig. 1a) shows that the SCM generates considerably less than the CRM. Convection is shallower in the SCM than in the CRM with convection in the SCM extending only to the tropopause height.

Out-of-cloud aircraft observations were used to estimate the state of the atmosphere prior to convection, while in-cloud observations were used to ensure that the CRM simulation reasonably represented convective transport. Due to differences in

scale, these observations are not intended for direct comparison with the model profiles but are presented in Figure 1b in order to provide information about the conditions used to construct the initial CO₂ profile and evaluate the CRM performance. Averaging CRM results over a 150 km by 150 km area yields a CO₂ profile verified with available observations which is directly comparable to the SCM results.

The initial condition profile of CO₂ (Figure 1b) shows the maximum CO₂ mixing ratios near the top of the boundary layer with lower mixing ratios below. Pollution from nearby Munich is likely responsible for enhancing CO₂ mixing ratios throughout the boundary layer while photosynthesis results in some CO₂ depletion near the surface. Despite a significant difference in CO₂ mixing ratios in the boundary layer (from 367 to 372 ppmv) and the free troposphere (from 363 to 365 ppmv), profiles of CO₂ mixing ratios calculated by both the CRM and SCM at the end of the 3-hour simulations show little change from the initial condition profile (Figure 1b). In the SCM, the lack of noticeable change in the CO₂ profile following convection is due to the relatively weak convective mass flux, though most of the air is being entrained into the storm near the altitude of peak CO₂ mixing ratios. In contrast, because the CRM entrains mass over a deeper layer from 1 to 3 km, much of the air entering the storm has lower mixing ratios reflecting the conditions above 1.5 km. When averaged over a large area of the CRM domain, little increase in upper tropospheric mixing ratios is seen even though a wide range of mixing ratios are present in the 150 km by 150 km area.

3.2 The July 10 STERAO storm

The STERAO-A (Stratospheric-Tropospheric Experiment: Radiation, Aerosols, and Ozone – Deep Convection and the Composition of the Upper Troposphere and Lower Stratosphere; Dye et al., 2000; Stenchikov et al., 2005) field campaign was

conducted in June and July of 1996. The field project included two research aircraft. The NOAA WP-3D flew below 8 km in order to characterize the chemical environment in which storms developed, while the University of North Dakota Citation sampled the meteorological and chemical properties of thunderstorm anvils. On July 10, 1996, at approximately 2100 UTC, a multicellular thunderstorm organized in a NW-SE line developed near the Wyoming-Nebraska border. The storm anvil was investigated by the Citation aircraft from 2237 to 0105 UTC including a spiraling ascent in the anvil from 0024 to 0050 UTC. After 0115 UTC, the storm transitioned to a unicellular structure and displayed supercell characteristics [Dye et al., 2000].

The July 10 STERAO storm has been the subject of several modeling studies [e.g. Skamarock et al. 2000; 2003; Barth et al. 2007a] and also serves as the basis of a cloud-scale model intercomparison by Barth et al. [2007b]. The storm was simulated by eight different CRMs, including the GCE and CSCTM, using identical initial conditions and the results compared with radar and in-cloud aircraft observations. The intercomparison found that the GCE, along with the other models, reasonably simulated the major storm features including the peak updraft velocities and storm structure. A comparison of aircraft observations from two cross-anvil transects and simulated CO and O₃ mixing ratios showed that the CSCTM driven by GCE output was able to reproduce the range of observations taken in the anvil region.

As in the July 21 EULINOX storm, the 3-hour SCM simulation of the July 10 STERAO storm produced significantly less convective mass flux (Figure 2a). The entrainment of air into the storm occurred in a shallower layer than in the CRM simulation and detrainment in the SCM convection occurred lower than in the CRM. The average CO profile calculated from CRM output at the end of the simulation shows a

maximum enhancement of approximately 20 ppbv in CO mixing ratios in the upper troposphere following convection (Figure 2b) while the SCM profile shows a smaller increase at these altitudes. An SCM simulation which omitted advective tendencies suggests that most of the increase in CO above 11 km is due to horizontal advection.

3.3 The July 3 CRYSTAL-FACE storm

The CRYSTAL-FACE (Ridley et al., 2004; Lopez et al., 2006) field campaign was conducted in July, 2002 over South Florida. Six research aircraft were involved in the project, including the NASA WB-57 which measured microphysical, chemical, and meteorological properties of tropical cirrus anvils in the vicinity of the tropopause, and the Twin Otter which sampled the chemical environment below 4 km. A variety of observations, including radar, lidar, and rawinsonde, were provided by land-based stations.

On July 3, 2002, convection developed along the west coast of Florida at approximately 1600 UTC. At 1700 UTC, convective cells began to develop in the middle of the Florida peninsula and along a sea breeze front on the east coast. The area in and above anvils associated with convection along the southeast coast was sampled by the WB57 from 1800-1945 UTC. Figure 3 shows an image from the NPOL Doppler radar at 1930, approximately 210 minutes after convection began along the west coast. From 1939 to 1945 UTC, the ER-2 aircraft made a west-to-east pass above the southern portion of the convective system. Images from the EDOP cloud radar aboard the ER-2 show precipitation top heights of 13.5 km.

The July 3 CRYSTAL-FACE storm was simulated by the NASA Goddard version of the MM5 with a horizontal resolution of 2 km and vertical resolution of 0.5 km. Fields from the NCEP Eta model at 00 UTC were used to initialize the model domain and

boundary conditions derived from the Eta fields were updated at 3-hour intervals.

Because the simulation from 000 to 1800 UTC was considered spin-up, only the MM5 output from 1800 to 2400 UTC was used in comparisons with radar observations and tracer transport calculations.

The MM5 simulation captured many of the observed features of the July 3 CRYSTAL-FACE storm. Simulated convective cells are evident along the west coast of Florida at 1800 UTC while observed convection began along the west coast at 1600 UTC. In the simulation, these convective cells move east across the Florida peninsula and reach the east coast at approximately 2230 UTC (Figure 4). Observations show cells originating in the middle of the peninsula and along the east coast rather than propagating from the west coast as in the simulation. The simulated storms pass from the west to east coast in approximately 4.5 hours while approximately 3.5 hours elapsed between the beginning of the observed storms and the mature phase of the storms along the east coast. The size of the simulated convective system compares well with the observations at 1930 UTC (Figure 3), though the simulated system is located slightly north of the observed system. Cross sections through the southern portion of the simulated storm at 2240 UTC shows that precipitation top heights were 14 km, which is slightly higher than the observed precipitation top height of 13.5 between 1939 and 1945 UTC.

The period of greatest relevance in the observed storm is from 1600 to 2000 UTC, when cells developing across the Florida peninsula were sampled by the WB57 aircraft. In the MM5 simulation, convection begins at 1800 and is located along the east coast at 2300 UTC. As a result, tracer transport was calculated using the MM5 fields from this time interval. Initial condition profiles of CO and CO₂ were constructed using data from the ascent and descent of the WB57 and portions of the flight in clear air. Because WB57

observations of CO were not available below 6.5 km and Twin Otter CO measurements were not available on July 3, both the mean CRYSTAL-FACE CO profile compiled using Twin Otter and WB57 data, and output from a global CTM were used to produce the initial condition profile of CO.

In-cloud aircraft observations taken from 1843 to 1853 at approximately 13 km elevation were used to evaluate the performance of convective transport in the simulation. Observations were averaged over 14-sec intervals to reproduce the 2-km spatial resolution of the model. Simulated CO and CO₂ mixing ratios were sampled at 13 km in the region of the storm with computed radar reflectivity between 0 and 30 dBZ because flights during CRYSTAL-FACE typically sampled only the lower reflectivity anvil region. Model results from 2100 UTC were used because the simulated storms began 2 hours later than observed. Probability distribution functions (pdfs) were calculated for both simulated and observed CO and CO₂ mixing ratios and are shown in Figure 5. The pdfs of simulated and observed CO₂ show a small overestimation of the maximum observed values by the model, suggesting that simulated upward transport may be slightly stronger than transport in the observed storm. However, this conclusion is not supported by an analysis of the CO pdfs which suggest that the CRM is underestimating convective transport. This contrast is likely due to the lack of CO observations available below 6.5 km, leading to inadequately defined vertical gradients in this region in the initial condition profile. Because CO₂ observations were available from the surface to the tropopause to guide the construction of the initial CO₂ profile, the CO₂ pdfs represent a better indicator of the success of the simulated convective transport.

The SCM was run for 5 hours with initial conditions and forcing derived from the MM5 fields from 1800 to 2300 UTC. Convective mass flux was averaged over the final

270 minutes of both the CRM and SCM simulations. As in the two midlatitude storms presented in Sections 3.1 and 3.2, the SCM simulation produced significantly less convective mass flux than the CRM simulation (Figure 6a). Both the SCM and CRM simulations indicate a lower cloud base in the CRYSTAL-FACE storm than in the STERAO and EULINOX storms, likely due to greater moisture in the boundary layer over Florida. In the SCM simulation of the July 3 CRYSTAL-FACE storm, most air is entrained into the storm at approximately 0.5 km, while in the CRM simulation, air is entrained from near the surface to 2 km. Boundary layer mixing ratios of CO and CO₂ are decreased as air is transported upwards by convection in the CRM simulation. Mixing ratios of these species are enhanced over the background values from 7 to 13 km, the region in which air is detrained from the storm in the CRM mass flux profile.

Generally, the CRM profiles of CO and CO₂ compare well with the available observations at anvil levels. CRM tracer profiles shown are area averages at the end of the 300 minute simulation, while the aircraft observations were taken over the course of the WB57 flight which lasted from 1600 to 2130 UTC. The region of the peninsula in which convection was active was sampled from approximately 1650 to 1950, after which the plane sampled an area off the west coast of Florida before landing in Key West. Apparent differences in the simulated trace gas profiles and observations may be the result of these spatial and temporal differences. Loewenstein et al. [2003] found that the high CO mixing ratios observed at approximately 7 and 11 km on July 3 may have resulted from biomass burning or convective outflow from a previous storm. Elevated CO₂ mixing ratios at these levels likely have a similar origin. Because observations at these altitudes occurred only during the aircraft's ascent and descent out of Key West, it was not possible to determine if these values represented conditions over the Florida

peninsula where convection developed or a more localized plume. As a result, these values were not used in constructing initial condition profiles and are not expected to be reproduced by either the SCM or CRM simulations. Significantly weaker convective mass flux in the SCM simulation resulted in little convective transport of CO and CO₂. Peaks seen in the SCM profiles of these species at 12 km are largely the result of the advective tendencies which were derived from the CRM simulation.

4. Parameter Sensitivity

Comparisons of convective mass flux from the simulations of three storms showed that the convective mass flux produced by the SCM was substantially weaker than that from the CRMs. This results in less upward transport of trace gases from the boundary layer and can significantly affect mixing ratios in the mid and upper troposphere. To investigate the sensitivity of convective transport in the SCM to the values of parameters contained in the moist physics schemes, regional sensitivity analysis (RSA; Hornberger and Spear, 1981) was used. The implementation of this method follows closely that of Liu et al. [2004] who used a multiple criteria extension to RSA developed by Bastidas et al. [1999] to investigate parameter sensitivity in a coupled land-atmosphere model.

A simpler one-at-a-time screening was used to reduce the parameter space prior to the more rigorous and computationally intensive RSA as in Liu et al. [2004]. The current implementation of moist physics in GEOS-5 includes a total of 56 parameters, 20 used in the RAS convective scheme and 36 in the prognostic cloud scheme. Feasible ranges of the 56 parameters were determined based on the functions of each parameter and a review of relevant literature. To determine the sensitivity of each parameter, the SCM was run for each of the three storms with a single parameter perturbed while all other

parameters were held constant. Each parameter was perturbed at 10% intervals from the minimum to the maximum value of the feasible range. The 16 parameters whose perturbation resulted in a 1% or greater change in the time averaged vertically integrated convective mass flux of any storm were considered in the subsequent RSA. A list of these parameters, their default values, and feasible ranges is provided in Table 1.

Unlike the one-at-a-time approach in which one parameter is varied while others remain fixed, RSA involves simultaneous variation of all parameters which allows parameter interdependencies to be accounted for in the sensitivity analysis. A number of samples, or parameter sets, are selected at random from the designated feasible ranges and the SCM is run with each set. The RSA then requires some criteria to divide the samples into a behavioral class (containing those simulations which produce the most favorable results) and a non-behavioral class (containing the remaining simulations in the sample) with the goal of identifying parameter sets which produce the most favorable outcomes. For the purpose of evaluating convective transport, time averaged vertically integrated convective mass flux derived from the CRM simulations was used as a criteria because direct observations of convective mass flux are not possible. Samples are ranked based on their ability to reproduce the CRM mass flux and, following Bastidas et al. [1999] and Liu et al. [2004], an arbitrary rank threshold is used to partition samples into behavioral and non-behavioral classes. Cumulative parameter distributions are computed for both classes and the Kolmogorov-Smirnov (K-S) test is used to determine if these distributions are statistically different. If so, a parameter would be considered to be sensitive. As in Liu et al. [2004], the K-S test is repeated using 200 bootstrapped samples and the K-S test statistic used to indicate sensitivity is the median of the values obtained. The procedure is repeated with successively larger sample sizes until the number of

sensitive parameters stabilizes.

The lower the value of the K-S probability for a parameter, the higher the sensitivity. Liu et al. [2004] considered all parameters with a K-S probability less than 0.01 to be highly sensitive and all parameters with a probability greater than 0.05 to be insensitive. Parameters with probabilities between 0.01 and 0.05 were deemed somewhat sensitive for the purpose of identifying parameters to be included in calibration studies. In this study, we consider only parameters with a K-S probability less than 0.01 to be sensitive. This criterion provided the greatest stability and was sufficient for the purposes of identifying the most important parameters with respect to convective transport.

To evaluate the sensitivity of the results to the choice of rank threshold used for partitioning samples into behavioral and non-behavioral classes, several different rank values were tested. A rank of 20 was selected for these studies because it provided the greatest stability regardless of sample size in all cases. The results from the RSA of the three storms are presented in Figure 7. In the case of the July 21 EULINOX storm, the number of sensitive parameters stabilized with a sample size of 12,000. The five parameters identified as sensitive with respect to convective mass flux were RASAL1 and RASAL2 (used to determine the relaxation time scale), ACRITFAC (a factor used to compute the critical value of the cloud work function which determines the initiation of convection), BASE_REVAP_FAC (used to determine the amount of rain re-evaporated into the environment), and AUTO_CN (used in the calculation of the auto-conversion of convective condensate). The number of sensitive parameters in the July 10 STERAO storm stabilized using a sample size of 18,000 and identified 6 parameters as sensitive. In addition to the 5 sensitive parameters from the EULINOX simulations, the LAMBDA_FAC parameter (used to calculate the minimum entrainment rate) also

displayed sensitivity in the July 10 STERAO storm. RSA in the July 3 CRYSTAL-FACE storm stabilized at a sample size of 10,000. The MIN_DIAMETER parameter (used to calculate the maximum entrainment rate) was deemed to be sensitive in the CRYSTAL-FACE storm, along with the five parameters common to the STERAO and EULINOX analyses.

Comparing the distributions of parameters in the behavioral and non-behavioral classes can also provide insight into which values produce the most favorable results. In the three cases analyzed, the use of default parameter settings resulted in much weaker convection in SCM simulations than in CRM simulations of the same storms. Members of the behavioral class of SCM simulations contained altered parameter settings which effectively increased the convective mass flux. Values of the parameters RASAL1 and RASAL2 which produce short relaxation time scales yielded the best comparison with CRM simulated mass flux. Values of the BASE_REVAP_FAC close to the upper limit of 1 produced better comparisons with the CRM results than values near the lower limit of 0. Large values of BASE_REVAP_FAC correspond to a higher degree of evaporation of falling precipitation which increases moisture in the model domain and facilitates stronger and more sustained convection. Similarly, low values of the parameter AUTO_CN produce better results by reducing the auto-conversion of convective condensate and, consequently, precipitation. The critical value of the cloud work function, ACRITFAC, determines the threshold for the initiation of convective adjustment. Smaller values of ACRITFAC result in a greater number of plumes contributing to the net mass flux of the cloud ensemble, thereby increasing the convective mass flux. The sensitivity of the LAMBDA_FAC and MIN_DIAMETER parameters in individual storms indicates that the maximum and minimum values of the entrainment

rate may also influence convective mass flux in certain conditions.

To further explore the impact of parameter settings on convection, vertical trace gas and convective mass flux profiles were averaged for all simulations in the behavioral class. In the July 21 EULINOX storm, the behavioral profile of time averaged convective mass flux shows more entrainment than the CRM profile below 4 km (Figure 8a). As in the control SCM run, the majority of air is entrained into the storm from a shallow layer approximately 1 km above the ground. The behavioral mass flux profile shows detrainment occurring from 4 to 10.5 km while the CRM profile decreases slightly from 4 to 8.5 km, and then more rapidly above 8.5 km. The largest difference between the behavioral and CRM CO₂ profiles is seen in the 1 to 2.5 km region where CO₂ is depleted in the behavioral simulations due to the stronger SCM mass flux (Figure 8b). CO₂ mixing ratios are slightly larger from 4 to 8 km in the behavioral profile than in the CRM profile because more high CO₂ air is transported upward from the boundary layer and detrained at these levels. In this storm, parameter settings which result in increased convective mass flux do not seem to improve the comparison between the CRM and SCM CO₂ profiles. This arises from the difference in entrainment and detrainment levels in the CRM and SCM simulations.

The mean behavioral profile of time averaged mass flux for the July 10 STERAO storm (Figure 9a) is similar in shape to that of the July 21 EULINOX storm. Entrainment in the behavioral profile is greater than in the CRM simulation below 4 km. Detrainment begins at approximately 4 km in the behavioral SCM profile and occurs more rapidly near the top of the cloud, from 8 to 11 km. In contrast, the CRM simulation continues to entrain air into the storm up to 6.5 km and then detrains air up to 14 km. In the CO profiles (Figure 9b), the greater degree of low level entrainment in the behavioral

simulations results in an underestimation of the CRM CO mixing ratios from 1 to 4 km. Nearly constant CO mixing ratios from 3.5 to 4.5 km in the behavioral profile mark the transition from entrainment to detrainment as seen in the mass flux profile. A similar feature is not noticeable in the default SCM profile because of the much weaker convective mass flux. From 8 to 9 km, the behavioral simulations slightly overestimate CO mixing ratios with respect to the CRM due to the greater detrainment at these levels in the SCM simulations of the storm. From 9 to 11 km, the behavioral CO profile compares well with the CRM profile because of the increase in convective mass flux resulting from parameter changes. Above 11 km, both the behavioral and control CO profiles underestimate the CRM CO profile due to the shallower cloud produced by the SCM.

The mean behavioral profile of time averaged convective mass flux in the July 3 CRYSTAL-FACE storm shows that the SCM continues to underestimate mass flux relative to the CRM simulation even with altered parameter settings (Figure 10a). However, the increase in mass flux resulting from changes in parameter values improves the representation of both CO and CO₂ from 8 to 11.5 km because more air originating at low levels has been transported upwards (Figures 10b and c). The behavioral CO and CO₂ profiles also compare more favorably with the CRM below 3 km than the SCM control simulation profiles.

5. Summary and Conclusions

Many evaluations of meteorological aspects of convection parameterizations have been presented in the past, often comparing SCM results with CRM results which are more easily validated against observations and can provide detailed information on cloud processes. This study extends that approach to examine the vertical distributions of trace

gases and convective mass flux produced by a SCM during three convective events observed during field projects. Because cloud mass flux, the quantity used by CTMs and GCMs to calculate convective transport, can not be observed, it is necessary to use CRMs as a proxy for observations. A comparison of radar observations and CRM output showed that the simulations were able to reproduce the dynamical evolution and structure of the observed storms. CRMs are also useful as a means of interpreting aircraft observations which represent both in- and out-of-cloud chemical environments that may differ substantially. Comparison of CRM results with in-cloud chemical measurements shows that in all three cases presented, the CSCTM was successful in reasonably representing convectively modified CO and CO₂ distributions.

The GEOS-5 SCM was used to simulate the selected storms using initial condition and forcing profiles of temperature, moisture, and trace gas mixing ratios computed by averaging over an area in the CRM domain comparable in size to a GCM gridcell. When default parameter values were used in the moist physics schemes, the SCM significantly underestimated convective mass flux relative to the CRMs which resulted in weaker transport of trace gases. In addition, clouds in the SCM were shallower than in the CRMs which has been noted in several previous studies. Pickering et al. [1995] compared convective mass fluxes produced by the GEOS-1 data assimilation system employing the RAS convective scheme with fluxes from a 2-D GCE simulation of a large squall line observed over Oklahoma during the PRE-STORM campaign. While the magnitudes of the profiles were similar, the GCE simulation produced greater mass flux at upper levels. Park et al. [2001] used a single-column chemical transport model driven with GEOS-1 convective mass fluxes to study the convective transport of ozone precursors. The transport of CO during the PRE-STORM squall line was compared with

2-D CRM results from Pickering et al. [1992] and showed that the altitude of maximum CO mixing ratios in the upper troposphere was 2 km lower in the column model than in the CRM, though no chemical observations were available to verify either simulation.

This work also presents an adaptation of a statistical technique for examining parameter sensitivity from earlier work by Liu et al. [2004] which identified the most significant parameters affecting ground temperature and surface fluxes in a coupled land-atmosphere SCM. This is the first study to examine the impact of parameter sensitivity on vertical trace gas distributions. The RSA identified five parameters as sensitive in all three case studies. These parameters affect the relaxation time scale in the RAS convective scheme, the amount of falling precipitation which is re-evaporated into the environment, the auto-conversion of convective condensate, and the critical value of the cloud work function. The results show that alterations to parameter settings can substantially improve the comparison between SCM and CRM convective mass flux with little impact on state variables. Modified parameter settings also improved the comparison between upper tropospheric trace gas mixing ratios in the SCM and CRM simulations of the STERAO and CRYSTAL-FACE storms. However, parameter settings do not significantly affect the depth of convective systems which results in detrainment at lower altitudes in the SCM than in the CRM. In the EULINOX storm, differences in the entrainment and detrainment levels between the CRM and SCM simulations resulted in poorer agreement between the models when the mass flux comparison was improved by modified parameter settings.

Perturbations to parameters which have been shown to exert the greatest control over convective transport will be used to construct an ensemble of global simulations representing the uncertainty introduced into simulated trace gas distributions by

convective schemes. Further investigation of the depth of convection in the GCM is also needed. This is especially significant because convective transport strongly influences the composition of the upper troposphere and lower stratosphere. Future GCM studies of long range pollution transport and climate change will be affected by the ability of convective parameterizations to realistically reproduce the depth of observed convection, as well as its intensity and location.

Despite some limitations, this approach offers new possibilities. Meteorological fields are relatively insensitive to many parameters used in the GCM, meaning there is often substantial leeway in setting these values. This study demonstrates that trace gases show sensitivity to convective parameters yielding an additional observational constraint. Future field and satellite campaigns which gather information on the vertical distributions of trace gases will provide the opportunity to use trace gas observations to further improve the representation of convective processes in global models.

Acknowledgments

Lesley Ott was supported through an ORAU postdoctoral fellowship. SCM research was funded by NASA's MAP program as part of a study to understand the distribution and transport of carbon species in the environment using GEOS-5. We thank Michele Rienecker for her support and encouragement to perform this research in the GMAO. CRM studies were supported under National Science Foundation grants ATM9912336 and ATM0004120 and NASA grant NAG5-11276. We thank Wei-Kuo Tao of NASA GSFC for supplying the 3-D GCE model and Alex DeCaria of Millersville University for assistance with the CSCTM. The EULINOX project was funded by the European Commission (Research DG) through the Environment and Climate program (contract

ENV4-CT97-0409). We thank the EULINOX team that carried out the airborne measurements (Schlager et al., DLR). We would also like to thank Karsten Baumann for providing observational data from the STERAO campaign; Yansen Wang, formerly of UMBC/JCET and currently at the US Army Research Center in Adelphi, MD, for providing the MM5 simulation of the July 3 CRYSTAL-FACE storm; and Paul Kucera, formerly of the University of North Dakota and currently at NCAR, for providing NPOL radar images of the July 3 CRYSTAL-FACE storm.

References

Arakawa, A., and W. H. Schubert, 1974: Interaction of a Cumulus Cloud Ensemble with the Large-Scale Environment, Part I, *J. Atmos. Sci.*, **31**, 674–701.

Bacmeister J. T., 2005: Moist processes in the GEOS5 AGCM. [Available online at <http://gmao.gsfc.nasa.gov/systems/geos5/STRUCTURE/AGCM/Moist.php>].

Bacmeister, J. T., M. J. Suarez, and F. R. Robertson, 2006: Rain Reevaporation, Boundary Layer–Convection Interactions, and Pacific Rainfall Patterns in an AGCM, *J. Atmos. Sci.*, **63**, 3383–3403.

Barth, M. C., S.-W. Kim, W. C. Skamarock, A. L. Stuart, K. E. Pickering, and L. E. Ott, 2007a: Simulations of the redistribution of formaldehyde and peroxides in the July 10, 1996 STERAO deep convection storm, *J. Geophys. Res.*, **112**, D13310, doi:10.1029/2006JD008046.

Barth, M. C., S.-W. Kim, C. Wang, K. E. Pickering, L. E. Ott, G. Stenchikov, M.

- Leriche, S. Cautenet, J.-P. Pinty, Ch. Barthe, C. Mari, J. Helsdon, R. Farley, A. M. Fridlind, A. S. Ackerman, V. Spiridonov, and B. Telenta, 2007b: Cloud-scale model intercomparison of chemical constituent transport in deep convection, *Atmos. Chem. Phys.*, **7**, 4709-4731.
- Bastidas, L. A., H. V. Gupta, S. Sorooshian, W. J. Shuttleworth, and Z. L. Yang, 1999: Sensitivity analysis of a land surface scheme using multicriteria methods, *J. Geophys. Res.*, **104**, 19,481–19,490.
- Bechtold P., et al., 2000: A GCSS intercomparison for a tropical squall line observed during TOGA-COARE. II: Intercomparison of single-column models and a cloud-resolving model, *Quart. J. Roy. Meteor. Soc.*, **126**, 865–888.
- Bey I., D. J. Jacob, J. A. Logan, and R. M. Yantosca, 2001: Asian chemical outflow to the Pacific: origins, pathways and budgets, *J. Geophys. Res.*, **106**, 23,097-23,114.
- DeCaria, A. J., 2000: *Effects of convection and lightning on tropospheric chemistry studied with cloud, transport, and chemistry models*, PhD dissertation, University of Maryland, College Park, 169 pp.

- DeCaria, A. J., K. E. Pickering, G. L. Stenchikov, and L. E. Ott, 2005: Lightning-generated NO_x and its impact on tropospheric ozone production: A three-dimensional modeling study of a Stratospher-Troposphere Experiment: Radiation, Aerosols, and Ozone (STERAO-A) thunderstorm, *J. Geophys. Res.*, **110**, D14303, doi:10.1029/2004JD005556.
- Dickerson, R.R., et al., 1987: Thunderstorms – an important mechanism in the transport of air pollutants, *Science*, **235**, 460–464.
- Dye, J. E., et al., 2000: An Overview of the STERAO--Deep Convection Experiment with Results for the 10 July Storm, *J. Geophys. Res.*, **105**, 10,023-10,045.
- Fehr, T., H. Höller, and H. Huntrieser, 2004: Model study on production and transport of lightning-produced NO_x in a EULINOX supercell storm, *J. Geophys. Res.*, **109**, D09102, doi:10.1029/2003JD003935.
- Folkens, I., P. Bernath, C. Boone, L. J. Donner, A. Eldering, G. Lesins, R. V. Martin, B.-M. Sinnhuber, and K. Walker (2006): Testing convective parameterizations with tropical measurements of HNO_3 , CO, H_2O , and O_3 : Implications for the water vapor budget, *J. Geophys. Res.*, **111**, D23304, doi:10.1029/2006JD007325.
- Höller, H., and U. Schumann, 2000: *EULINOX – The European Lightning Nitrogen Oxides Project*, Rep. DLR-FB 2000-28, Deutsches Zentrum für Luft- und Raumfahrt, Köln, pp. 240.

Höller, H., H. Huntrieser, C. Feigl, C. Théry, P. Laroche, U. Finke, and J. Seltmann, 2000: The Severe Storms of 21 July 1998 – Evolution and Implications for NO_x-Production, in *EULINOX – The European Lightning Nitrogen Oxides Experiment*, edited by H. Höller and U. Schumann, *Rep. DLR-FB 2000-28*, Deutsches Zentrum für Luft- und Raumfahrt, Köln, pp. 109-128.

Hornberger, G. M. and R. C. Spear, 1981: An approach to the preliminary analysis of environmental systems, *J. of Environ. Manage.*, **12**, 7-18.

Huntrieser, H., et al., 2002: Airborne measurements of NO_x, tracer species, and small particles during the European Lightning Nitrogen Oxides Experiment, *J. Geophys. Res.*, **107**, 4113, doi:10.1029/2000JD000209.

Liu, Y., H. V. Gupta, S. Sorooshian, L. A. Bastidas, and W. J. Shuttleworth, 2004: Exploring parameter sensitivities of the land surface using a locally coupled land-atmosphere model, *J. Geophys. Res.*, **109**, doi:10.1029/2004JD004730.

Lock, A. P., A. R. Brown, M. R. Bush, G. M. Martin, and R. N. B. Smith, 2000: A New Boundary Layer Mixing Scheme. Part I: Scheme Description and Single-Column Model Tests, *Mon. Wea. Rev.*, **128**, 3187–3199.

- Loewenstein, M., H. J. Jost, J. P. Lopez, J. R. Podolske, E. Richards, K. Aiken, A. Stohl, N. Spichtinger, D. Murphy, D. Cziczo, 2003: Biomass burning signatures in CO observed during CRYSTAL-FACE, *presented at the CRYSTAL-FACE Science Team Meeting*, Salt Lake City, Utah.
- Lopez, J. P., et al., 2006: CO signatures in subtropical convective clouds and anvils during CRYSTAL-FACE: An analysis of convective transport and entrainment using observations and a cloud-resolving model, *J. Geophys. Res.*, **111**, doi:10.1029/2005JD006104.
- Louis, J.-F., 1979: A parametric model of vertical eddy fluxes in the atmosphere, *Bound.-Layer Meteor.*, **17**, 187–202.
- Luo, Y., S. K. Krueger, and K. M. Xu, 2006: Cloud Properties Simulated by a Single-Column Model. Part II: Evaluation of Cumulus Detrainment and Ice-Phase Microphysics Using a Cloud-Resolving Model. *J. Atmos. Sci.*, **63**, 2831–2847.
- Moorthi, S., and M. J. Suarez, 1992: Relaxed Arakawa–Schubert: A parameterization of moist convection for general circulation models, *Mon. Wea. Rev.*, **120**, 978–1002.
- Ott, L. E., K. E. Pickering, G. L. Stenchikov, H. Huntrieser, and U. Schumann, 2007: Effects of lightning NO_x production during the 21 July European Lightning Nitrogen Oxides Project storm studied with a three-dimensional cloud-scale chemical transport model, *J. Geophys. Res.*, **112**, doi:10.1029/2006JD007365.

- Park, R. J., G. L. Stenchikov, K. E. Pickering, R. R. Dickerson, D. J. Allen, and S. Kondragunta, 2001: Regional air pollution and its radiative forcing: Studies with a single-column chemical and radiation transport model, *J. Geophys. Res.*, **106**, 28,751–28,770.
- Pickering, K. E., A. M. Thompson, J. R. Scala, W.-K. Tao, R. R. Dickerson, and J. Simpson, 1992: Free tropospheric ozone production following entrainment of urban plumes into deep convection, *J. Geophys. Res.*, **97**, 17,985–18,000.
- Pickering, K. E., A. M. Thompson, W.-K. Tao, R. B. Rood, D. P. McNamara, and A. M. Molod, 1995: Vertical transport by convective clouds: Comparisons of three modeling approaches, *Geophys. Res. Lett.*, **22**, 1089–1092.
- Pickering, K. E., et al., 1996: Convective transport of biomass burning emissions over Brazil during TRACE A, *J. Geophys. Res.*, **101**, 23,993–24,012.
- Ridley B. A., et al., 2004: Florida thunderstorms: A faucet of reactive nitrogen to the upper troposphere, *Journal of Geophysical Research*, **109**, doi:10.1029/2004JD004769.

Rienecker, M. M., M. J. Suarez, R. Todling, J. Bacmeister, L. Takacs, H.-C. Liu, W. Gu, M. Sienkiewicz, R. D. Koster, R. Gelaro, and I. Stajner., 2007: The GEOS-5 Data Assimilation System - Documentation of Versions 5.0.1 and 5.1.0. /NASA TM 104606, Technical Report Series on Global Modeling and Data Assimilation/, *v27*.

Ryan, B. F., J. J. Katzfey, D. J. Abbs, C. Jakob, U. Lohmann, B. Rockel, L. D. Rotstain, R. E. Stewart, K. K. Szeto, G. Tselioudis, and M. K. Yau, 2000: Simulations of a cold front by cloud-resolving, limited-area, and large-scale models, and a model evaluation using in situ and satellite observations, *Mon. Wea. Rev.*, **128**, 3218–3235.

Simpson, J., and V. Wiggert, 1969: Models of precipitating cumulus towers, *Mon Weath Rev.*, **97**, 471-489.

Skamarock, W. C., et al., 2000: Numerical simulations of the July 10 Stratospheric-Tropospheric Experiment: Radiation, Aerosols, and Ozone/Deep Convection Experiment convective system: Kinematics and transport, *J. Geophys. Res.*, **105**, 19,973–19,990.

Skamarock, W. C., J. E. Dye, E. Defer, M. C. Barth, J. L. Stith, B. A. Ridley, K. Baumann, 2003: Observational- and modeling-based budget of lightning-produced NO_x in a continental thunderstorm, *J. Geophys. Res.*, **108**, doi:10.1029/2002JD002163.

- Stenchikov, G., R. Dickerson, K. Pickering, W. Ellis, B. Doddridge, S. Kondragunta, O. Poulida, J. Scala, W.-K. Tao, 1996: Stratosphere-Troposphere Exchange in a Mid-Latitude Mesoscale Convective Complex: Part 2, Numerical Simulations, *J. Geophys. Res.*, **101**, 6837-6851.
- Stenchikov., G., K. Pickering, A. DeCaria, W.-K. Tao, J. Scala, L. Ott, D. Bartels, T. Matejka, 2005: Simulation of the fine structure of the July 12, 1996 STERAO-A storm accounting for effects of terrain and interaction with mesoscale flow, *J. Geophys. Res.*, **110**, doi:10.1029/2004JD005582.
- Strahan, S. E., A. R. Douglass, J. E. Nielsen, and K. A. Boering, 1998: The CO₂ seasonal cycle as a tracer of transport, *J. Geophys. Res.*, **103**, 13729-13741.
- Tao, W.-K., and J. Simpson, 1993: Goddard Cumulus Ensemble Model. Part I: Model description, *Terr., Atmos., Oceanic Sci.*, **4**, 35-72.
- Tao, W.-K., J. Simpson, D. Baker, S. Braun, M.-D. Chou, B. Ferrier, D. Johnson, A. Khain, S. Lang, B. Lynn, C.-L. Shie, D. Starr, C.-H. Sui, Y. Wang and P. Wetzel, 2003a: Microphysics, Radiation and Surface Processes in the Goddard Cumulus Ensemble (GCE) Model, *Meteorology and Atmospheric Physics*, **82**, 97-137.
- Tao, W.-K., et al., 2003b: Regional-scale modeling at NASA Goddard Space Flight Center, *Research Signpost - Recent Res. Devel. Atmos. Sci.*, **2**, 1-52.

Waliser, D. E., J. A. Ridout, S. Xie, and M. Zhang, 2002: Variational Objective Analysis for Atmospheric Field Programs: A Model Assessment, *J. Atmos. Sci.*, **59**, 3436–3456.

Xu, K. M., 1995: Partitioning Mass, Heat, and Moisture Budgets of Explicitly Simulated Cumulus Ensembles into Convective and Stratiform Components. *J. Atmos. Sci.*, **52**, 551–573.

Zhu Y. and R. Gelaro, 2007: Observation sensitivity calculations using the adjoint of the Gridpoint Statistical Interpolation (GSI) analysis system. *Mon. Wea. Rev.* (submitted).

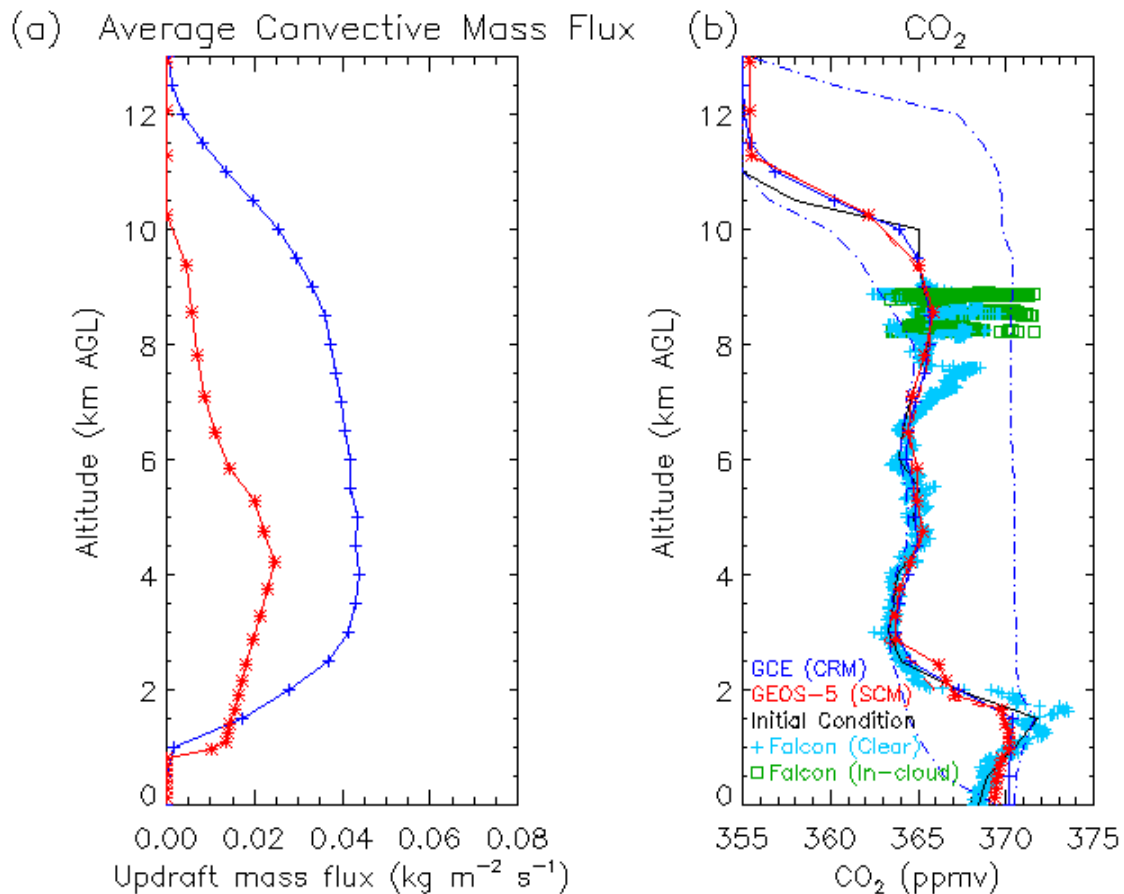


Figure 1. (a) Convective mass flux from CRM (blue) and SCM (red) simulations of the July 21 EULINOX storm, averaged over 150 minutes. (b) CO₂ mixing ratios at the end of the 3-hour CRM and SCM simulations compared with CO₂ observations from the Falcon aircraft. Solid (dashed) red line shows SCM CO₂ calculated with (without) advective tendencies calculated from the CRM. The solid blue line indicates CRM results averaged over a 150 km by 150 km region while the dash-dot blue lines show the maximum and minimum values within the averaging area. Plus signs (squares) represent observations from the Falcon aircraft taken outside (inside) of the cloud.

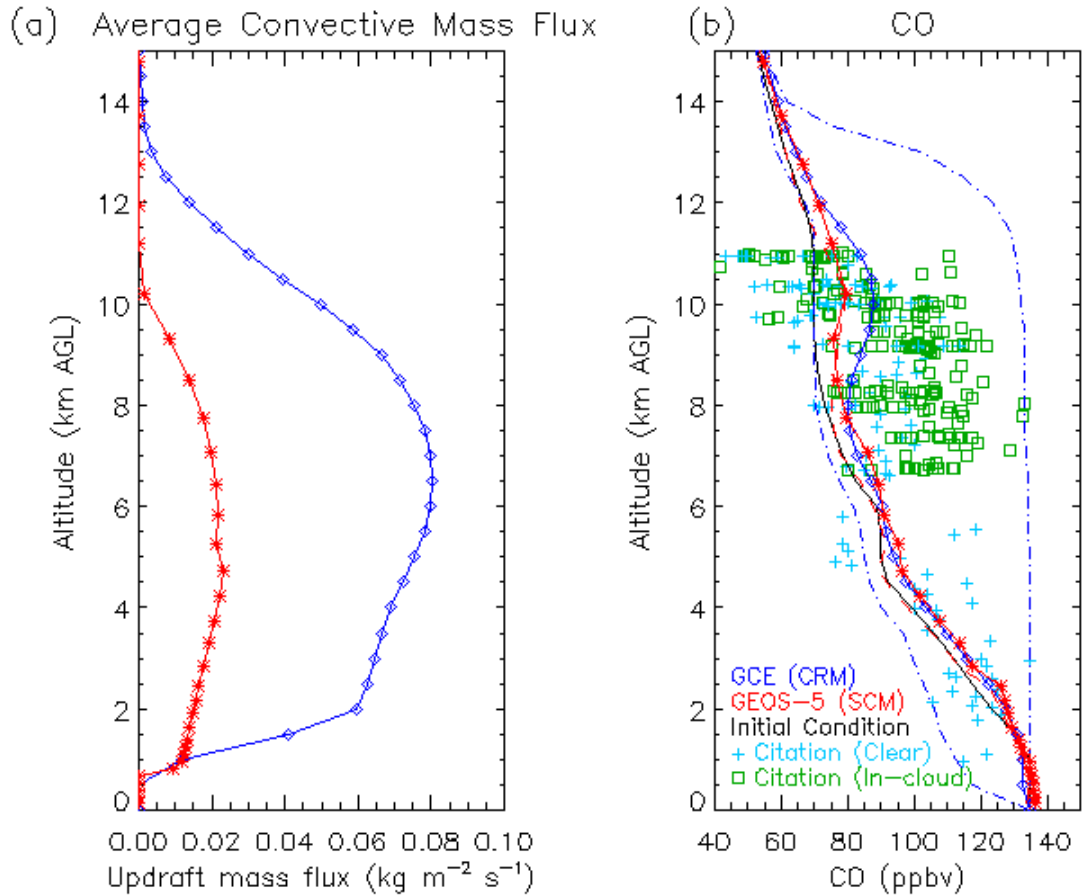


Figure 2. (a) Convective mass flux from CRM (blue) and SCM (red) simulations of the July 10 STERAO storm, averaged over 150 minutes. (b) CO mixing ratios at the end of the 3-hour CRM and SCM simulations compared with CO observations from the Citation aircraft. Solid (dashed) red line shows SCM CO calculated with (without) advective tendencies calculated from the CRM. The solid blue line indicates CRM results averaged over a 150 km by 150 km region while the dash-dot blue lines show the maximum and minimum values within the averaging area. Plus signs (squares) represent observations from the Citation aircraft taken outside (inside) of the cloud.

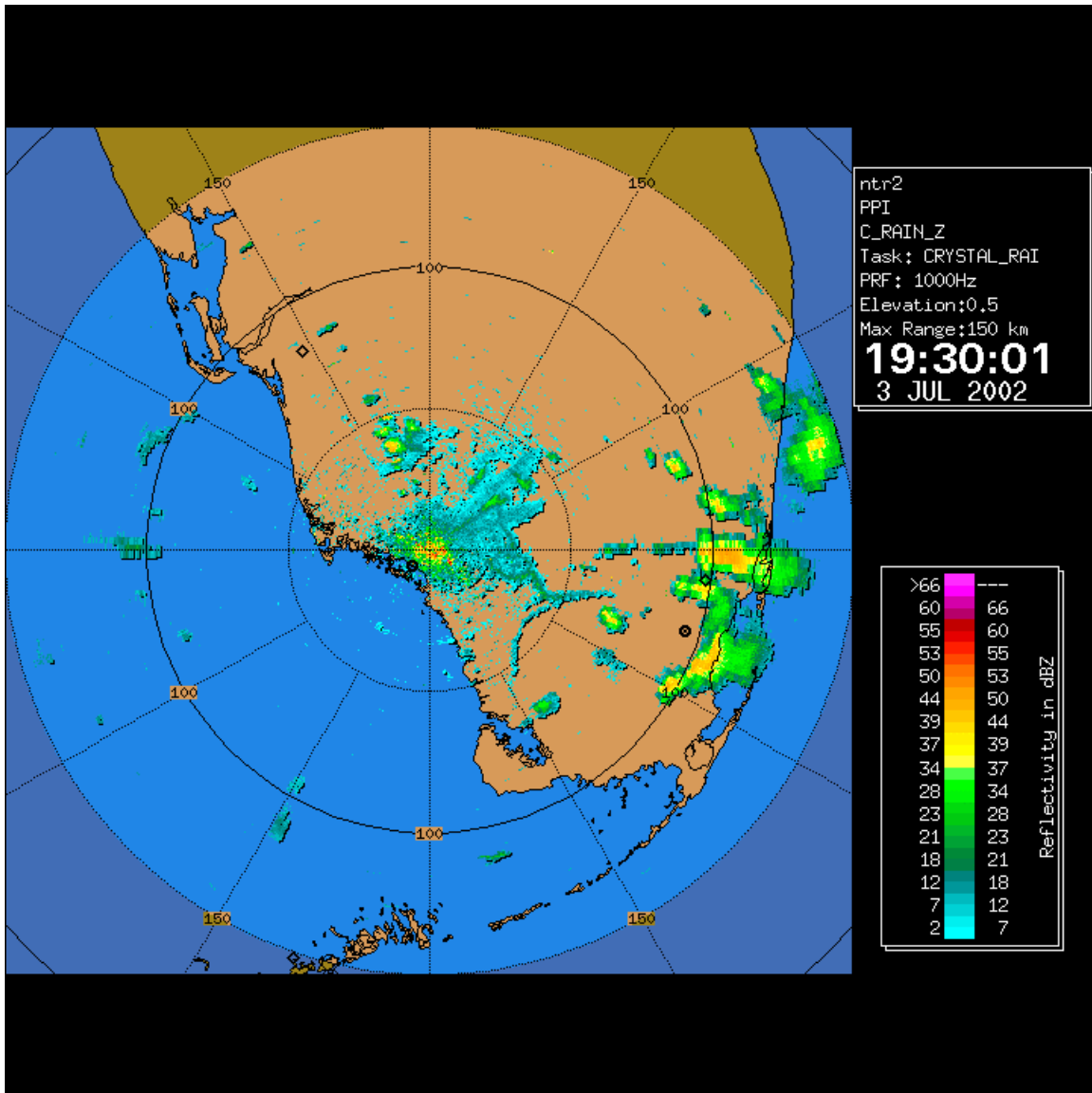


Figure 3. CAPPI reflectivity image from the NPOL Doppler radar located at the CRYSTAL-FACE western ground site near Everglades City, Florida at 1930 UTC on July 3, 2002 at 0.5 km.

Radar Reflectivity(dBZ) Z = 0.5 km 2230 UTC

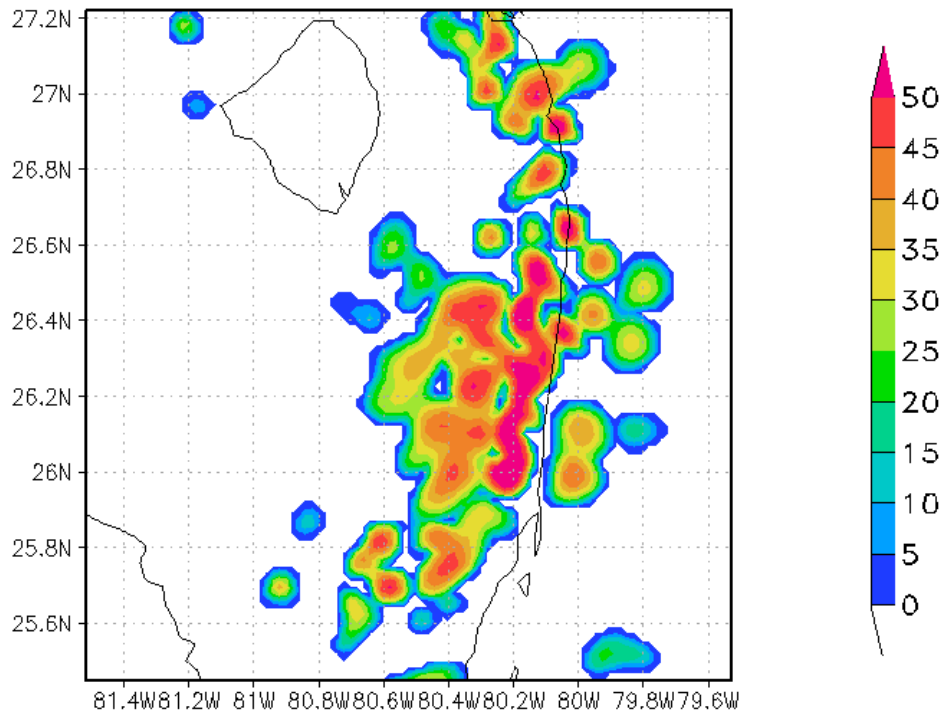


Figure 4. Radar reflectivity at 0.5 km calculated from MM5 simulated hydrometeor fields at 2230 UTC during the July 3 CRYSTAL-FACE storm.

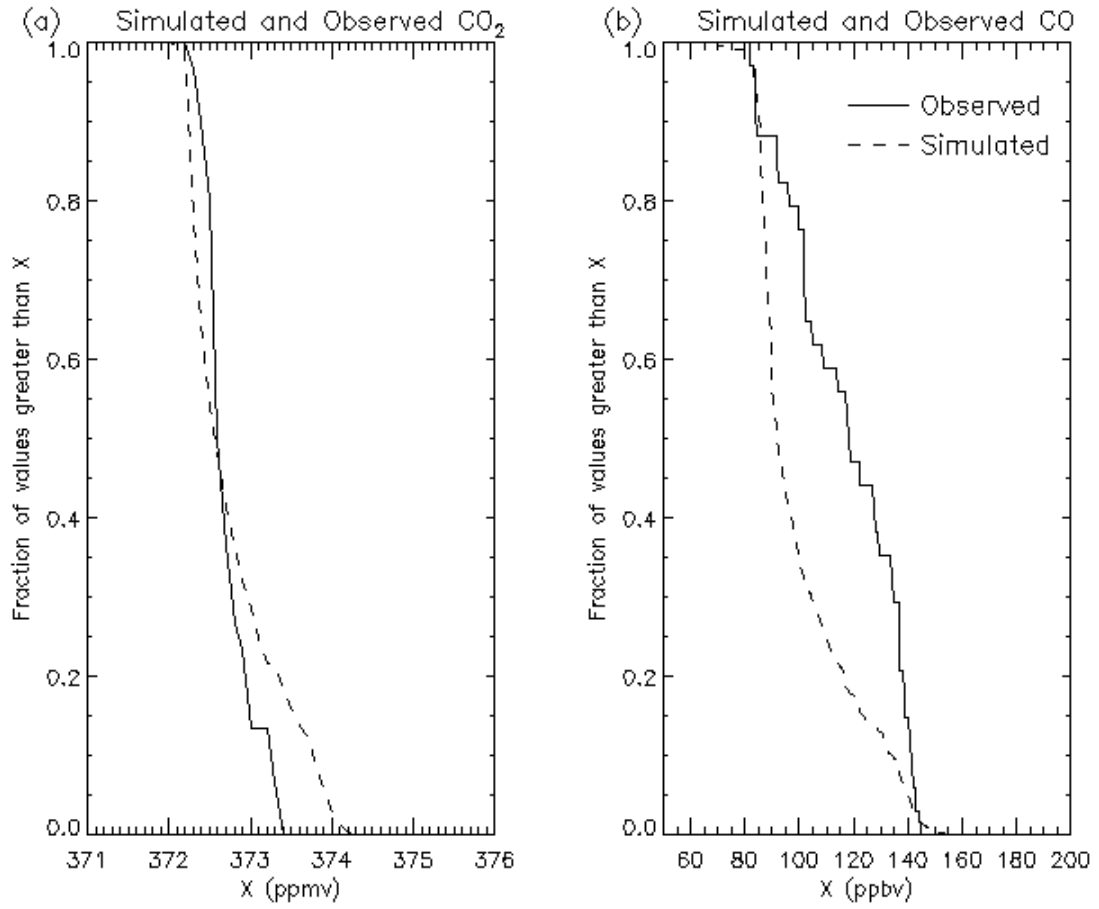


Figure 5. Pdfs of simulated (dashed) and observed (solid) CO (a) and CO₂ (b) at 13 km AGL in the July 3 CRYSTAL-FACE storm.

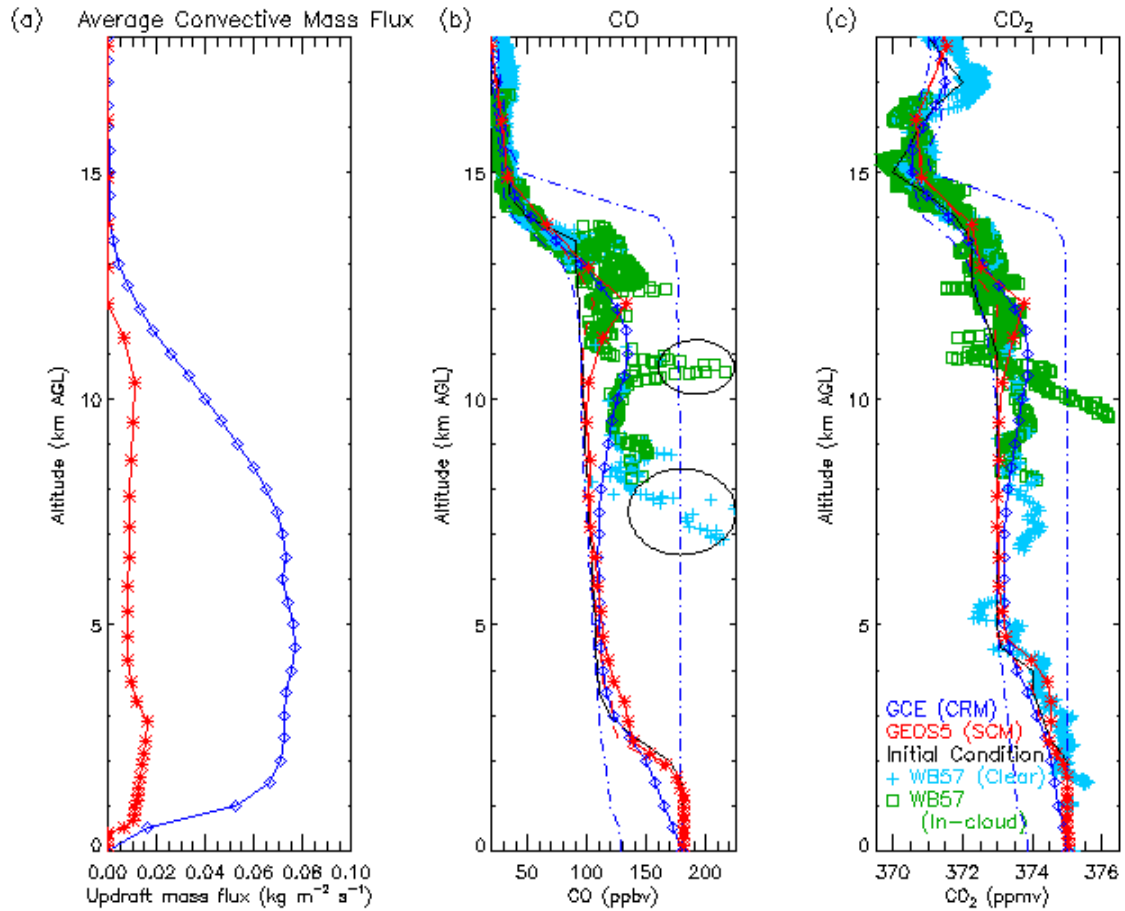


Figure 6. (a) Convective mass flux from the CRM (blue) and SCM (red) simulations of the July 3 CRYSTAL-FACE storm averaged over 270 minutes. CO (b) and CO₂ (c) mixing ratios at the end of the 5-hour simulations compared with observations from the WB57 aircraft. Solid (dashed) red line shows SCM CO and CO₂ calculated with (without) advective tendencies calculated from the CRM. The solid blue line indicates CRM results averaged over a 150 km by 150 km region while the dash-dot blue lines show the maximum and minimum values within the averaging area. Plus signs (squares) represent aircraft observations from the WB57 taken outside (inside) of the cloud. Circled areas in (b) indicate measurements which may be influenced by biomass burning or outflow from a previous convective event.

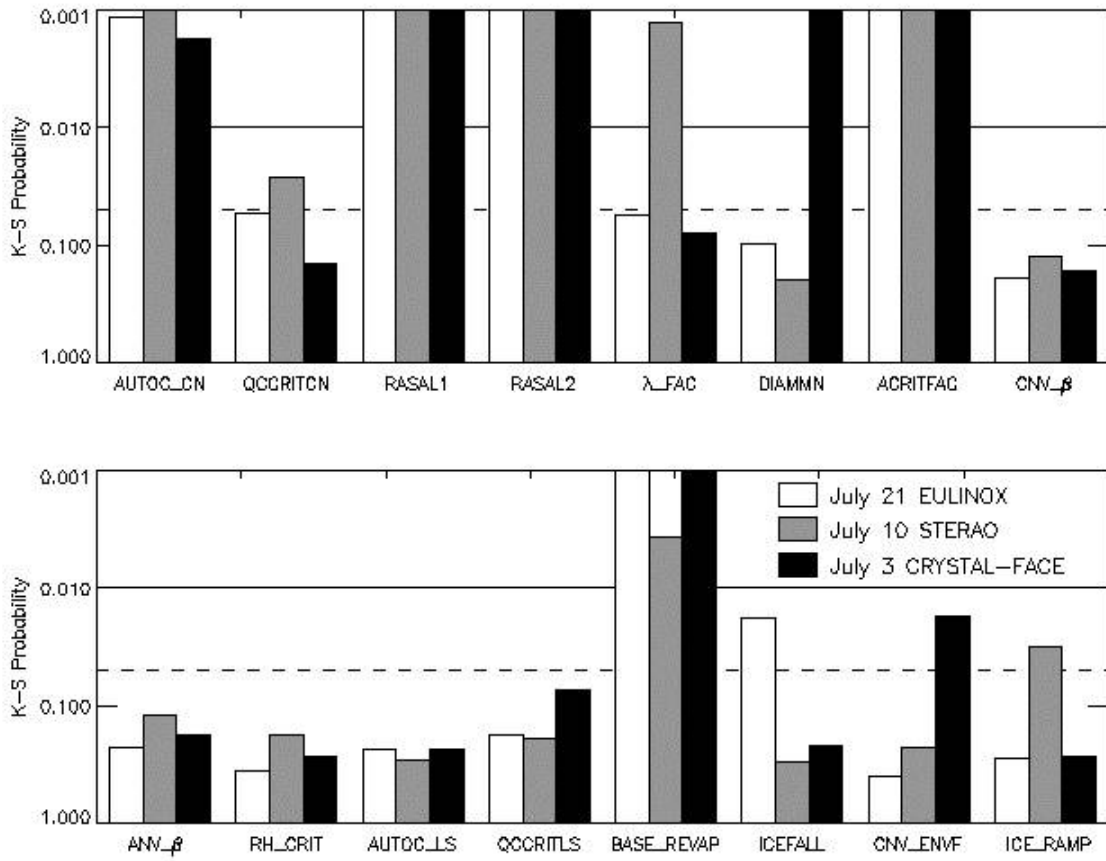


Figure 7. K-S probabilities computed from RSA for 16 parameters listed in Table 1 for the EULINOX (white), STERAO (gray), and CRYSTAL-FACE (black) storms. Solid line indicates the threshold for determining sensitive parameters. Dashed line designates somewhat sensitive criteria from Liu et al. [2004].

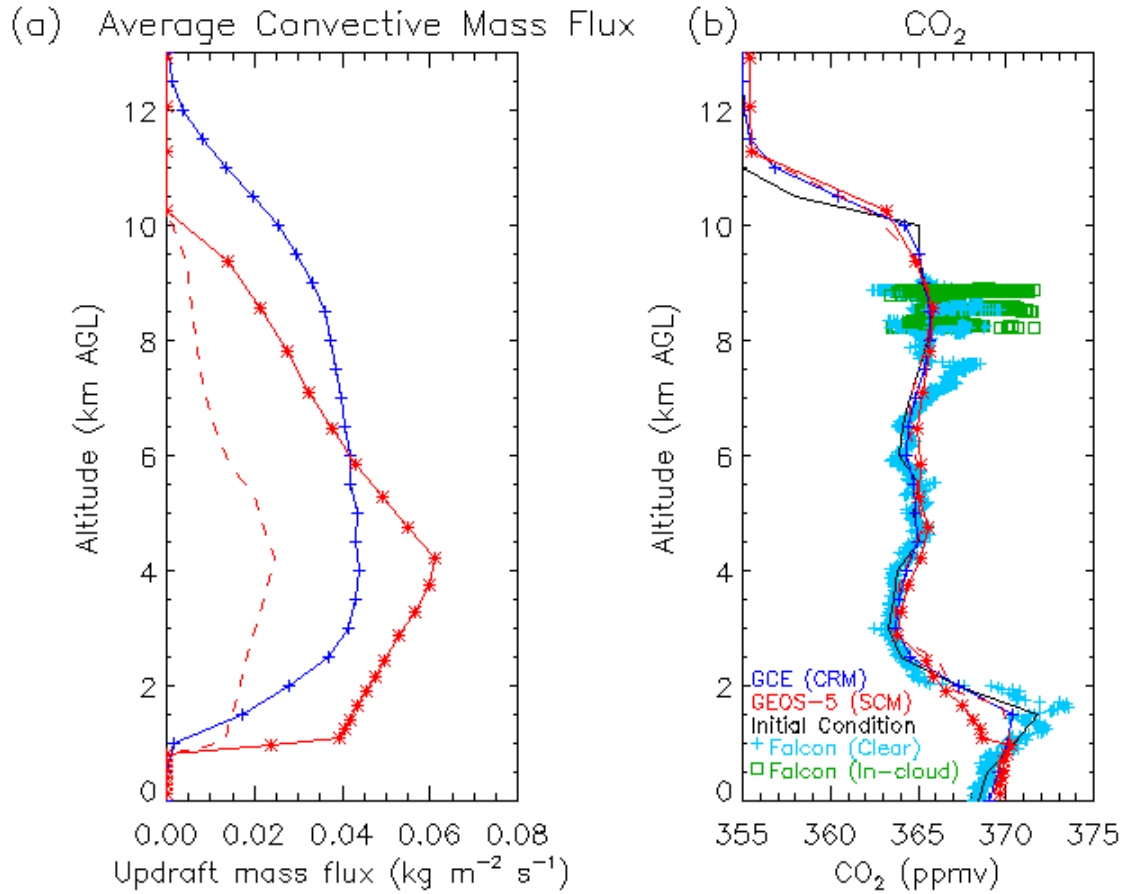


Figure 8. Vertical profiles of convective mass flux (a) and CO₂ (b) from CRM (blue) and SCM (red) simulations of the July 21 EULINOX storm. Solid red lines represent the average over all simulations in the behavioral class while dashed red lines represent the control simulation assuming default parameter settings. Mass flux profiles are averaged over 150 minutes. CO₂ mixing ratios are calculated at the end of the 3-hour simulations and compared with CO₂ observations from the Falcon aircraft.

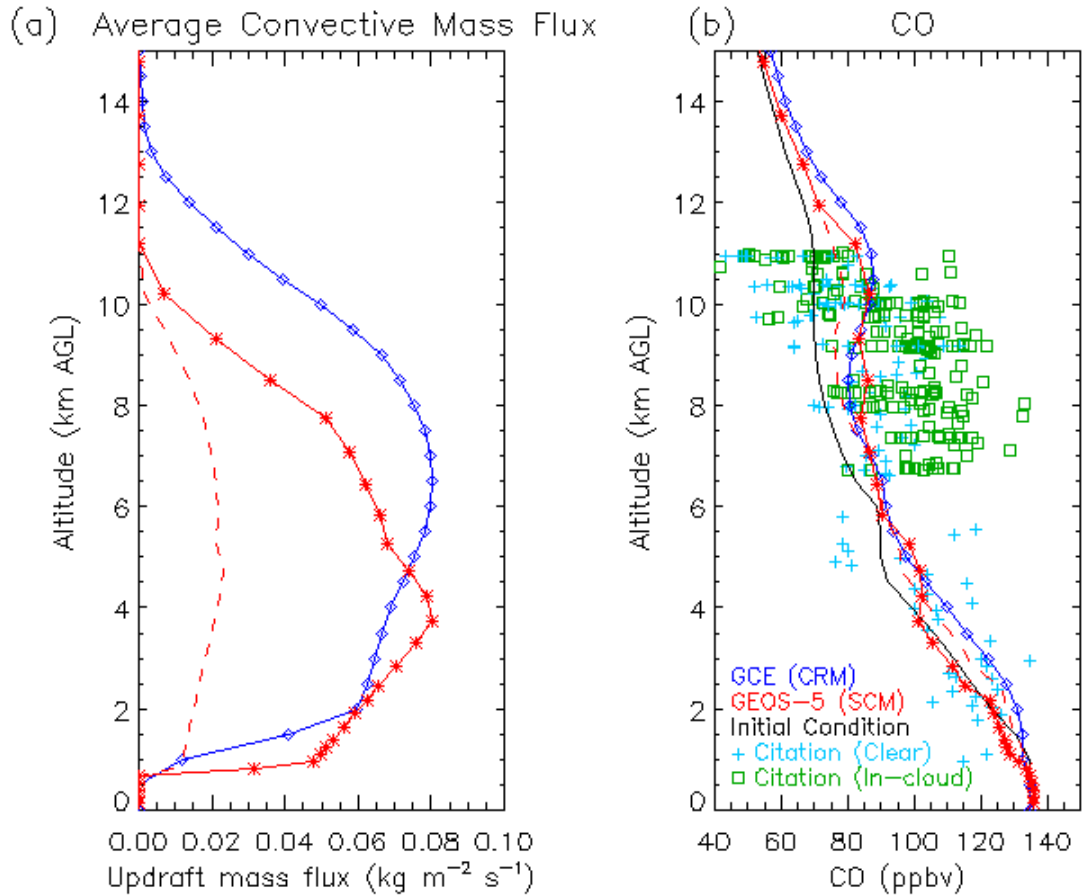


Figure 9. Vertical profiles of convective mass flux (a) and CO (b) from CRM (blue) and SCM (red) simulations of the July 10 STERAO storm. Solid red lines represent the average over all simulations in the behavioral class while dashed red lines represent the control simulation assuming default parameter settings. Mass flux profiles are averaged over 150 minutes. CO mixing ratios are calculated at the end of the 3-hour simulations and compared with CO observations from the Citation aircraft.

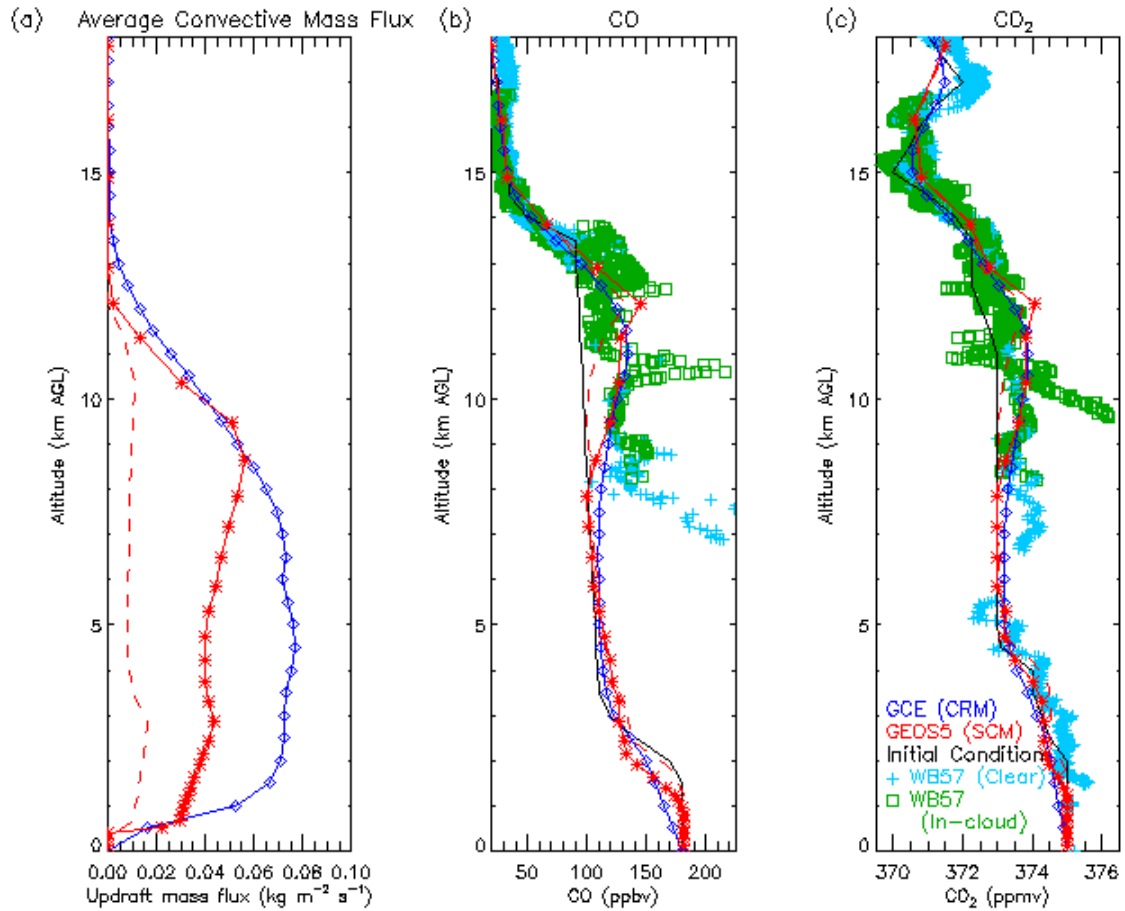


Figure 10. Vertical profiles of convective mass flux (a), CO (b), and CO₂ (c) from CRM (blue) and SCM (red) simulations of the July 3 CRYSTAL-FACE storm. Solid red lines represent the average over all simulations in the behavioral class while dashed red lines represent the control simulation assuming default parameter settings. Mass flux profiles are averaged over 270 minutes. CO and CO₂ mixing ratios are calculated at the end of the 5-hour simulations and compared with observations from the WB57 aircraft.

RAS Parameters	Default	Minimum	Maximum	Description
AUTO_CN	2.50E-003	1.00E-004	1.00E-002	Maximum autoconversion rate (1/s) for convective condensate
QC_CRIT_CN	8.00E-004	1.00E-004	1.00E-002	Critical value (g/g) for autoconversion of convective condensate
RASAL1	1800	1800	1.00E+005	Minimum convective relaxation time scale (s). Used for shallow clouds (tops<2km)
RASAL2	1.00E+005	1800	1.00E+005	Maximum convective relaxation time scale (s). Used for deep clouds (tops~10km)
LAMBDA_FAC	4	1	10	Ratio of maximum cloud diameter to subcloud layer thickness. Controls minimum entrainment rate
MIN_DIAMETER	200	100	300	Minimum cloud diameter (m). Determines maximum entrainment rate via Simpson relation.
ACRITFAC	0.5	0.1	1	Scaling factor for critical cloud work function
Prognostic Cloud Parameters				
CNV_BETA	10	0.1	10	Scaling factor for area of convective rain showers
ANV_BETA	4	0.1	10	Scaling factor for area of showers falling from anvil clouds
RH_CRIT	0.95	0.95	1	Critical relative humidity for cloud formation
AUTO_LS	2.00E-003	1.00E-004	1.00E-002	Maximum autoconversion rate (1/s) for large scale condensate
QC_CRIT_LS	8.00E-004	1.00E-004	1.00E-002	Critical value (g/g) for autoconversion of large-scale condensate
BASE_REVAP_FAC	1	0	1	Fraction of estimated rain re-evaporation actually applied
ANV_ICEFALL	1	0.1	1	Scaling parameter for sedimentation velocity of cloud ice
CNV_ENVF	0.8	0.1	1	Fraction of precipitation assumed to fall through environment.
ICE_RAMP	-40	-60	-20	Temperature (C) below which newly formed condensate is assumed to be pure ice.

Table 1. Selected physics parameters varied in this study. Default values in the GEOS-5 SCM as well as minimum and maximum values used here are given. Parameters AUTO_CN and QC_CRIT_CN are used in Sundquist type expressions for autoconversion (Bacmeister et al 2006). Entrainment rates (1/m) in RAS are assumed to be related to an imagined cloud radius R according to $\frac{1}{M} \frac{dM}{dz} = \frac{0.2}{R}$ as in Simpson and Wiggert (1969).